

# QUALITY EVALUATION OF PROGRESSIVE LOSSY-TO-LOSSLESS REMOTE-SENSING IMAGE CODING

Ian Blanes, Joan Serra-Sagristà

Dept. of Information and Communications Engineering  
Universitat Autònoma de Barcelona (Spain)

## ABSTRACT

Progressive lossy-to-lossless methods for hyper-spectral image coding are becoming common in remote-sensing. However, as remote-sensing imagery is sometimes fed directly into an automated process, there are several alternative distortion measures directed to quantify the image quality with regard to how this process will perform. In this scenario, we investigate the quality evolution in the lossy regime of progressive lossy-to-lossless and perform a detailed evaluation.

**Index Terms**— Hyper-spectral image coding, progressive lossy-to-lossless, remote sensing, quality evaluation, multi-component JPEG2000

## 1. INTRODUCTION

Techniques that allow Progressive Lossy-to-Lossless (PLL) are gaining traction in the Remote Sensing (RS) community. This is because, in moderate bitrates, they have similar Rate-Distortion (R-D) performances to lossy techniques, and, on lossless, they yield Compression-Ratios (CRs) competitive with pure lossless methods. Moreover, they also allow for embedded bitstreams, where bitrate reduction can be performed by selecting a subset of the original bitstream.

Unlike in other areas, in RS a lossy image is not always consumed by visual inspection, but by some kind of automated process. This is especially true for hyper-spectral imagery, and for this reason a moderate amount of alternative quality measures have appeared in the last years. As its purpose is to quantify future information extraction from an image, they are referred to as Information Extraction Measures (IEMs).

However, to the best of the authors' knowledge, the lossy regime of PLL methods has yet to be examined with those measures.

PLL methods have been known for a long time [1], but it is just recently that its use on hyper-spectral imagery has started

---

This work was supported in part by the Spanish and Catalan Governments, and by FEDER, under grants TS12006-14005-C02-01, SGR2005-00319, and FPU2008. Computational resources used in this work were partially provided by the Oliba Project of the Universitat Autònoma de Barcelona.

to extend, in part because of the improvements in reversible spectral transforms. Reviews of PLL for RS can be found in [2, 3]. As for IEMs, a comprehensive review can be found in [4].

This paper is organized as follows. First, common setups for PLL encoding are discussed in Section 2. IEMs are detailed in Section 3. Experimental results follow in Section 4. And finally, conclusions close this paper.

## 2. PROGRESSIVE LOSSY-TO-LOSSLESS CODING

PLL encoders have structures similar to the ones from lossy coders. The differences arise in that each stage is replaced by a lossless equivalent, and then a lossless bitstream can be produced by encoding all bitplanes. As in lossy coding, if applied to hyper-spectral imagery, a spectral decorrelation is prefixed to the process and Volumetric R-D is taken into account.

Common techniques for PLL are JPEG2000 and *Tarp-based coding with Classification for Embedding* [3]. Both of them allow for lossy or lossless stages, and both yield similar performances [3]. With regard to lossless spectral transforms, two are the common choices: the well known Integer Wavelet Transform (IWT) and the Reversible Karhunen-Loève Transform (RKLT). The latter, first proposed in [5], is a lossless approximation of the Karhunen-Loève Transform (KLT). As with the IWT, the lifting structure is used to ensure reversibility. A new multilevel clustered approach has been recently proposed [6]. It substantially reduces the computation time and has the same CRs and R-D properties (see Fig. 1). In the sequel, this variant of the RKLT will be used.

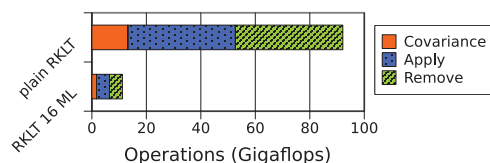


**Fig. 1:** Operation count of the Multi-level Clustered RKLT compared to the plain RKLT.

### 3. INFORMATION EXTRACTION MEASURES

This section describes several hyper-spectral measures oriented to quantitatively assess the performance of an automated information extraction process.

Measures presented have been grouped in two categories. The first category includes measures that try to evaluate qualities from a statistical point of view, and the second includes measures directly linked to the output of classification processes.

For brevity of description,  $I$  will denote the original image,  $I_z$  will denote the component  $z$  of the original image, and this same convention will be extended to the recovered image  $R$ .

The measures included in the first category are:

#### Maximum Spectral Similarity (MSS) [7]

$$MSS = \max_{x,y} \left\{ \sqrt{\frac{\|I_{x,y} - R_{x,y}\|_2^2}{size_z} + (1 - \rho_{x,y}^2)^2} \right\}$$

where

$$\rho_{x,y} = \frac{\sigma(I_{x,y}, R_{x,y})}{\sigma(I_{x,y})\sigma(R_{x,y})}$$

and  $\sigma$  is the sample variance or covariance function.

It is used to ensure class homogeneity in an unsupervised classifier. It measures changes in spectral magnitude and direction.

#### Maximum Spectral Angle (MSA)

$$MSA = \max_{x,y} \left\{ \cos^{-1} \left( \frac{\langle I_{x,y}, R_{x,y} \rangle}{\|I_{x,y}\|_2 \cdot \|R_{x,y}\|_2} \right) \right\}$$

The MSA quantifies the peak angular distortion. It is brightness invariant, and is usually presented in degrees.

#### Spectral Wang-Bovik Q [8, 4]

$$Q_\lambda = \min_{x,y} \{Q(I_{x,y}, R_{x,y})\}$$

$$Q_{stack} = \min_z \{Q(I_z, R_z)\}$$

where

$$Q(U, V) = \frac{4\sigma(U, V)\mu(U)\mu(V)}{(\sigma(U)^2 + \sigma(V)^2)(\mu(U)^2 + \mu(V)^2)}$$

and  $\mu$  is the mean function.

It is intended to evaluate the distortion in the three following properties: correlation, luminance, and contrast.

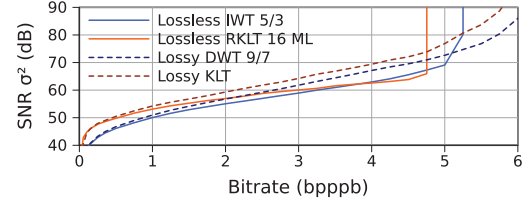


Fig. 2: R-D comparison of PLL and lossy methods.

On the second category, measures are based on the distortion between classification results. A common way to quantify these results is the Preservation of Classification (POC), where the percentage of spatial locations that maintain the same class are counted. Two common unsupervised classification methods used for this purpose are the k-means classification and the Reed Xiaoli (RX) anomaly detection algorithms.

**k-Means classification** k-Means is a very common clustering approach [9]. In this case, the spectral angle has been selected as classification distance for its brightness invariance, and the number of desired cluster has been set to 10.

**RX anomaly detection** This is also a very common procedure in remote sensing [10]. While the direct application is very straightforward, it requires the inverse of the spectral covariance matrix, which does not always exist. We recommend alternative methods based on the computation of the Mahalanobis distance in the KLT space [11]. As for the threshold selection, we will consider the top 1% locations to be anomalies.

All these measures have been implemented in an open source package available at [12].

## 4. EXPERIMENTAL RESULTS

Experimental results are performed on the widely available AVIRIS corpus by NASA [13]. The usual top-left tile of  $512 \times 512$  pixels is selected. Images are stored as 16 bit signed integers. Unless otherwise stated, results are presented for Cuprite, and other images yielded similar results.

Encodings have been performed with both spectral transforms described, and JPEG2000<sup>1</sup> with Mean Squared Error (MSE) as R-D optimization distance.

First, Signal-to-Noise Ratio (SNR) and CR results will be shown so the reader can assess qualities by traditional means. In Fig. 2, PLL methods are compared with their lossy counterparts. As can be observed, similar results are obtained up to a 1 bpppb, and then PLL versions start to decline. However, around 5 bpppb, PLL methods become lossless. In Table 1, a comparative of the target bitrates for lossless compression

<sup>1</sup>JPEG2000 encodings have been performed with Kakadu Software [14]

	IWT	RKLT	M-CALIC	LUT
Cuprite	5.28	4.86	4.86	4.61
Jasper Ridge	5.54	4.87	4.96	4.92
Low Altitude	5.95	5.21	-	-
Lunar Lake	5.30	4.96	4.96	4.77
Moffett Field	5.65	4.98	5.05	5.13
Yellowstone	4.79	3.89	-	-

**Table 1:** Comparison of target bitrate for lossless recovery between PLL and pure lossless methods. Pure lossless results from [3]. M-CALIC and LUT are introduced respectively in [15, 16].

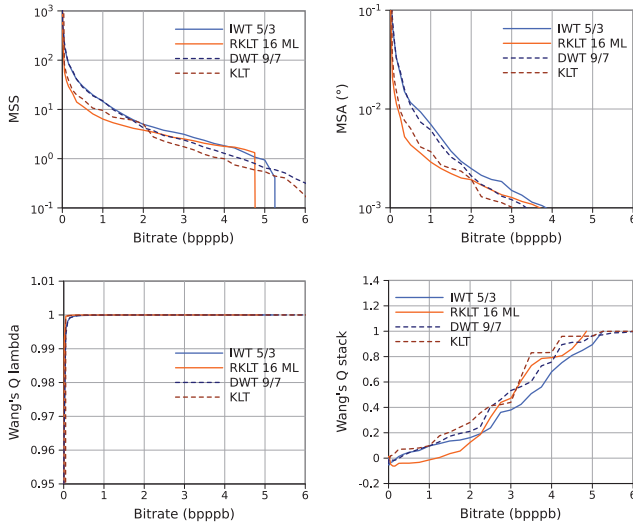


**Fig. 3:** Quality evolution for statistical measures. On MSS and MSA less is better, and on  $Q_s$  less is worse.

is presented. It can be appreciated that PLL yields similar results to other pure-lossless state-of-the-art techniques.

Once the traditional properties of PLL have been established, results from IEMs will be presented. Using the same convention as in Section 3, results for statistical measures will be presented first.

In Fig. 3 plots for all the statistical IEMs are shown. All measures, but  $Q_\lambda$ , have large graceful decays and no instabilities, which is good. However,  $Q_{stack}$ , saturates around 5 bpppb, even for lossy techniques.  $Q_\lambda$  has a large constant zone, and is insensitive to large amounts of compression. This leads to doubt about the usefulness of this specific  $Q$  extension to spectral images.

Regarding classification-related metrics, plots for quality evolution are provided in Fig. 4, and visual inspections in Fig. 5 and Fig. 6.

In these experiments, k-means has proved to be very resistant to high amounts of compression, losing less than 2% of performance at 0.5 bpppb. From visual inspection, we see that most of the spatial locations that change class are located

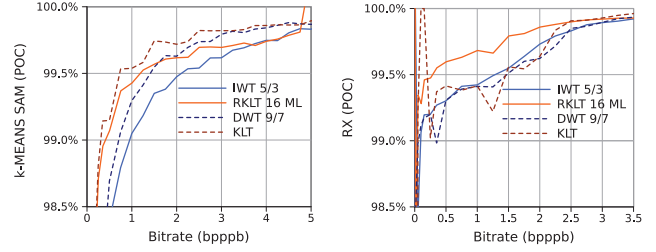


**Fig. 4:** Quality evolution for classification-based measures. RX anomaly threshold is 1%.

	Correlation
RMSE and MSS	0.998
RMSE and MSA	0.988
MSS and MSA	0.983
$Q_{stack}$ and Real Bitrate	0.985

**Table 2:** Measure correlation for Cuprite compressed with RKLT and JPEG2000. The other images yielded similar results.

on the boundaries, and that a high structural similarity is still preserved.

RX, on the other hand, is very sensitive to compression. Compression up to 1 bpppb still preserves most of the original features, but as compression increases, strong artifacts appear. And, on very low bitrates, the algorithm is extremely unstable and becomes unusable. As shown, the RKLT provides a substantial improvement over the other methods. Also note, that although RX performances might seem similar to the ones of k-means, the high bias between classes and the small number of them make a 0.5% error ratio, change half of the anomalies detected.

To conclude this experimental analysis we investigated the correlation between these metrics and the “traditional” ones, in order to detect measures with similar responses to distortion introduced by compression. Correlation between two measures has been computed, for each image, by sampling the compression process at bitrates from 0.25 bpppb to 11.75 bpppb in intervals of 0.25 bpppb. Most relevant results are provided in Table 2. Strong correlations ( $\rho > 0.95$ ) have been found between MSS, MSA, and the square root of the MSE. Also, an interesting result is the high correlation between  $Q_{stack}$  and the real bitrate achieved by the encoder.

On the other hand, no apparent relation has been found involving classification-based metrics. In addition, we have seen that using other distances on the k-means algorithm, such as the Euler distance or the Manhattan distance, produces similar results ( $\rho > 0.99$  between them).

## 5. CONCLUSIONS AND FUTURE RESEARCH

In this paper, after an overview of the current state of Progressive Lossy-to-Lossless (PLL) encoders for hyper-spectral

imagery, a detailed investigation of the lossy regime of PLL encoders evaluated with alternative measures is presented.

First, traditional properties of PLL encoders are assessed, showing both good SNR at moderate bitrates, and good CR at lossless.

Two families of alternative measures are presented: the statistical family, where statistical properties of an image are used to infer distortion; and the classification-based family where distortion is linked to the performance of an unsupervised classifier.

On the statistical family, measures are found to highly correlate with already known properties of the coding process (*i.e.* MSE and bitrate). Therefore, the analyzed measures of this family provide little value in this scenario. However, the reported correlation might only occur on the performed coding process, and other processes (fusion, sharpening, segmentation, Gaussian noise, ...) might not produce this correlation.

Quite the contrary, classification-based measures do not directly correlate into any other measures, even between them, and seem to provide a reliable threshold for compression. Furthermore, each one has a different tolerance to compression artifacts.

Future research on this topic might be the use of supervised classification-based measures or the extension of these results to other corpus of RS images, and other sources of distortion.

## 6. REFERENCES

- [1] A. Said and W.A. Pearlman, "An image multiresolution representation for lossless and lossy compression," *IEEE Trans. Image Process.*, vol. 5, no. 9, pp. 1303–1310, Sep. 1996.
- [2] G. Ginesu, D.D. Giusto, and W.A. Pearlman, "Lossy to lossless SPIHT-based volumetric image compression," *Proc. Int'l Conf. Acoust., Speech, Signal Process., 2004. (ICASSP 04).*, vol. 3, pp. iii–693–6 vol.3, May 2004.
- [3] J. Zhang, J. E. Fowler, and G. Liu, "Lossy-to-lossless compression of hyperspectral imagery using three-dimensional TCE and an integer KLT," *IEEE Geosci. Remote Sens. Lett.*, vol. 5, no. 4, pp. 814–818, Oct. 2008.
- [4] E. Christophe, D. Leger, and C. Mailhes, "Quality criteria benchmark for hyperspectral imagery," *IEEE Trans. Geosci. Remote Sens.*, vol. 43, no. 9, pp. 2103–2114, Sept. 2005.
- [5] P.W. Hao and Q.Y. Shi, "Reversible integer KLT for progressive-to-lossless compression of multiple component images," *Proc. 2003 Int'l Conf. Image Process. (ICIP 2003)*, vol. 1, pp. 633–636, Sept. 2003.
- [6] I. Blanes and J. Serra-Sagrà, "Clustered reversible-KLT for progressive lossy-to-lossless 3d image coding," in *Data Compression Conf. 2009 (DCC 2009)*. Mar. 2009, IEEE Press.
- [7] S.T. Rupert, M.H. Sharp, J.N. Sweet, and E.J. Cincotta, "Noise constrained hyperspectral data compression," *Int'l Geosci. Remote Sens. Symp. 2001. (IGARSS 01)*, vol. 1, pp. 94–96 vol.1, Jul. 2001.
- [8] Z. Wang and A.C. Bovik, "A universal image quality index," *IEEE Signal Process. Lett.*, vol. 9, no. 3, pp. 81–84, Mar. 2002.
- [9] J. B. MacQueen, "Some methods for classification and analysis of multivariate observations," in *Proc. 5th Berkeley Symp. Math. Statistics and Probability*, L. M. Le Cam and J. Neyman, Eds. 1967, vol. 1, pp. 281–297, University of California Press.
- [10] I.S. Reed and X. Yu, "Adaptive multiple-band CFAR detection of an optical pattern with unknown spectral distribution," *IEEE Trans. Acoust., Speech, Signal Process.*, vol. 38, no. 10, pp. 1760–1770, Oct. 1990.
- [11] R. De Maesschalck, D. Jouan-Rimbaud, and D. L. Massart, "The mahalanobis distance," *Chemometrics and Intelligent Laboratory Systems*, vol. 50, no. 1, pp. 1–18, 2000.
- [12] Group on Interactive Coding of Images, "Coding software," <http://gici.uab.cat/>, 2009.
- [13] Jet Propulsion Laboratory and NASA, "Airborne Visible InfraRed Imaging Spectrometer website," 1997, <http://aviris.jpl.nasa.gov/html/aviris.overview.html>.
- [14] D.S. Taubman, "Kakadu software," <http://www.kakadusoftware.com/>, 2000.
- [15] E. Magli, G. Olmo, and E. Quacchio, "Optimized onboard lossless and near-lossless compression of hyperspectral data using calic," *IEEE Geosci. Remote Sens. Lett.*, vol. 1, no. 1, pp. 21–25, Jan. 2004.
- [16] J. Mielikainen, "Lossless compression of hyperspectral images using lookup tables," *IEEE Signal Process. Lett.*, vol. 13, no. 3, pp. 157–160, Mar. 2006.

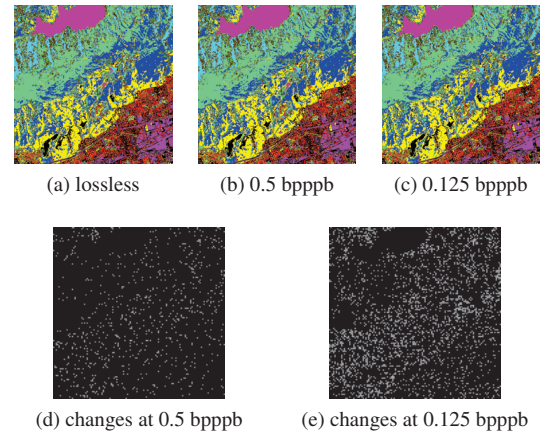


**Fig. 5:** Visual inspection of k-means classification for Moffett Field and RKL with JPEG2000.

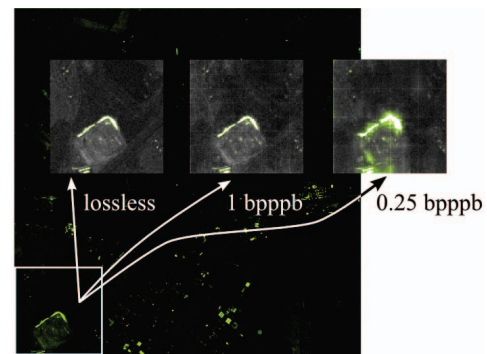


**Fig. 6:** Visual inspection of RX anomaly detection for Low Altitude and RKL with JPEG2000.